Food Chemistry: X 14 (2022) 100312

Contents lists available at ScienceDirect

Food Chemistry: X

journal homepage: www.sciencedirect.com/journal/food-chemistry-x

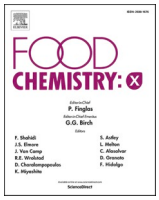

Co-encapsulation of chlorogenic acid and cinnamaldehyde essential oil in Pickering emulsion stablized by chitosan nanoparticles

Ben Niu [a,b,c,d], Hangjun Chen [a,b,c,d], Weijie Wu [a,b,c,d], Xiangjun Fang [a,b,c,d], Honglei Mu [a,b,c,d], Yanchao Han [a,b,c,d], Haiyan Gao [a,b,c,d,*]

[a] Food Science Institute, Key Laboratory of Post-Harvest Handling of Fruits, Ministry of Agriculture and Rural Affairs
[b] Key Laboratory of Fruits and Vegetables Postharvest and Processing Technology Research of Zhejiang Province
[c] Key Laboratory of Postharvest Preservation and Processing of Fruits and Vegetables, China National Light Industry
[d] Zhejiang Academy of Agricultural Sciences, Hangzhou 310021, China

ARTICLE INFO

Keywords:
Co-encapsulation
Pickering emulsion
Chitosan particles
Chlorogenic acid
Cinnamaldehyde essential oil

ABSTRACT

Most of the current research only explored the loading of an active substance in active packaging. In this study, cinnamaldehyde essential oil (CEO) and chlorogenic acid (CA) were co-encapsulated in chitosan (CS) nanoparticles based Pickering emulsion. The morphology and wettability of CS-CA particles were determined. In addition, physicochemical characterizations and stability of the Pickering emulsion were also investigated. Results showed that the wettability of nanoparticles was improved with increasing the ratios of CS to CA, which is helpful to stabilize the emulsion. CEO Pickering emulsion was stabilized by CS-CA nanoparticles and CEO emulsion showed the best stability by using CS-CA nanoparticles with the ratios of CS to CA 1:0.75 with the minimum creaming index value of 26.5 ± 4.6% after 5 days of storage. These overall results presented in this work demonstrate, for the first time, the potential of Pickering emulsion for the co-encapsulation of water-soluble and water-insoluble ingredients.

1. Introduction

Rise in global demand for fresh fruits and vegetables during the previous four decades associated mainly with income growth, and consumers' awareness from fresh foods nutritional and health benefits. (Lin, Lin, Lin, Fan, & Lin, 2021). However, fruits and vegetables have high water content, rich nutrition, and active metabolism (Liu, Gao, Chen, Fang, & Wu, 2019). All fresh fruits and vegetables are susceptible to oxidation and microbial infection during the harvest and storage process, resulting in shortened storage period of fruits and vegetables, and even deterioration and loss of edible value, causing economic losses and food safety issues (Gao, Fang, Chen, Qin, Xu, & Jin, 2017). Active packaging loaded antibacterial or antioxidant ingredient has been widely studied (Jiang, Liu, Fang, Tong, Chen, & Gao, 2022). However, most of the current research only explored the loading of an active substance in an active packaging. Theoretically speaking, active packaging loaded with antioxidant and antibacterial ingredients at same time can further prolong the shelf life of food products, especially for fruits and vegetables whose surfaces are prone to oxidative browning and microbial infection.

Cinnamaldehyde essential oil (CEO) is a kind of natural plant essential oil extracted from different parts of cinnamon such as branches, leaves and bark. Cinnamaldehyde is the representative active components of CEO. CEO has been used as antimicrobial agents to maintain quality and prolongs the shelf life of fresh fruits and vegetables (Liu et al., 2022). Chlorogenic acid (CA) represent a large family of phenolic compounds consisting of an ester formed from L-quinic acid and hydroxycinnamic acid, with axial hydroxyls on carbons 1 and 3 versus equatorial hydroxyls on carbons 4 and 5 (Valeria et al., 2019). As natural antioxidant agents, CA was drawing more and more attention in food preservation (Jiao, Shu, Li, Cao, Fan, & Jiang, 2019).

However, the present application of CEO and CA is restricted due to the environmental degradation (Cao et al., 2021). There is also a lack of mature technology to co-encapsulate CEO and CA. Pickering emulsion is universally applied in pharmacology, biomedicine, and food industries. In addition, Pickering emulsion can also be elaborately designed to improve the stability of bioactive substances. Most previous studies focused on the encapsulating of individual bioactive components in

* Corresponding author.
E-mail address: spsghy@163.com (H. Gao).

https://doi.org/10.1016/j.fochx.2022.100312
Received 10 February 2022; Received in revised form 1 April 2022; Accepted 13 April 2022
Available online 18 April 2022

nanoparticles at the oil–water interface or dispersed into the oil phase (Xia, Xue, & Wei, 2021). Few studies have been reported the simultaneous encapsulating of different soluble active ingredients into the emulsion.

Chitosan nanoparticles have long been used as carriers for controlled release of active substances and could also be used as an emulsion stabilizer (Rattanaburi, Charoenrat, Pongtharangkul, Suphantharika, & Wongkongkatep, 2019). The dissolved chitosan molecules lack interfacial activity and cannot be used directly to stabilize emulsions (Ho, Ooi, Mwangi, Leong, Tey, & Chan, 2016). Chitosan nanoparticles can be prepared by pH-regulated self-aggregation, ionic gelation, polyelectrolyte complexation and hydrophobic modification, which can improve the wettability of chitosan, and then Pickering emulsions could be stabilized by CS nanoparticles (Ribeiro et al., 2020). The aim of this study is to co-encapsulate oil-soluble essential oil and water-soluble CA in Pickering emulsion system. Different amount of chlorogenic acid was encapsulated into CS nanoparticles by ionic crosslinking with tripolyphosphate (TPP). The physicochemical characterizations including microscopic observation, particle size and water contact angle of particles were determined. Then Pickering emulsion system stabilized by CS-CA nanoparticles with different ratios was prepared. In addition, physicochemical characterizations and stability of emulsion were also investigated. The information in our research will provide basic knowledge about CS nanoparticles and the results obtained by quantitative analysis in this paper will be useful for the subsequent application of co-encapsulating Pickering emulsion.

2. Materials and methods

2.1. Materials

Chitosan (degree of deacetylation≈95%; molecular weight≈10 kDa) was purchased from Yuanye Bio-Technology Co., Ltd. (Shanghai,China). Cinnamaldehyde (purity: 95%) was purchased from Yuanye Bio-Technology Co., Ltd. (Shanghai,China). Chlorogenic acid (purity: 95%) was purchased from Aladdin Chemistry Co., Ltd. (Shanghai, China). Sodium tripolyphosphate (TPP) was bought from Sinopharm Chemical Reagent Co., Ltd. (Shanghai, China). All chemicals were in analytical grade unless specified.

2.2. Preparation of chitosan nanoparticles

CS-CA nanoparticles were prepared based on the ionic cross-linking of chitosan with Sodium tripolyphosphate (TPP) according to the method of Nallamuthu with some modifications (Nallamuthu, Devi, & Khanum, 2015). Briefly, CS solution 0.5% (w/v) was made by dissolving 0.5 g CS in 100 mL aqueous acetic acid solution. After that, 20 mL CS solution was transferred to another beaker and pH was adjusted to 4.6 by using 2 mol/L of NaOH. Various amount of CA were added to CS solution to obtain 1:0.25, 1:0.5, 1:0.75, 1:1 wt ratios of CS to CA. The mixed solution was stirred for 5 h in the dark. Subsequently, 50 mL TPP solution (1 mg/mL) was added drop wise to mixed CS-CA solution under magnetic stirring. The same procedure without CA addition was applied for the preparation of CS particles. Then freshly prepared particles were obtained and collected by centrifugation at 10,000 × g for 35 min at 4 °C. Eventually, the freshly prepared particles were dispersed in 25 mL of water to produce a uniform suspension with ultrasound assisted treatment.

2.3. Characterization of CA-loaded CS nanoparticles

2.3.1. Microscopic observation of CA-loaded CS nanoparticles

Scanning electron microscope (TM3000, Hitachi, Tokyo, Japan) was used for the morphological characterization of the nanoparticles. The freshly formed nanoparticles were diluted with purified water, and a drop of the diluted dispersion was dried on tin foil at room temperature. Then, the dried sample was sputter-coated with gold for better conductivity before examined.

2.3.2. Particle size, polydispersity index (PdI) and zeta (ζ)-potential

The Z-average diameter, zeta (ζ)-potential and polydispersity index (PDI) of the nanoparticles were measured according to Ben Niu et al. by using Malvern Mastersizer MS2000 (Malvern Instruments Ltd., Malvern, UK) (Niu, Shao, & Sun, 2019). Before measurement, nanoparticle dispersion was diluted with deionized water to an appropriate concentration and shaken for 2 min to avoid multiple scattering effects of the particles. Each sample was measured in triplicates.

2.3.3. Wettability measurement of chitosan nanoparticles

The contact angle measurements of CS nanoparticles and CS-CA nanoparticles were determined by Automatic Video Micro Contact Angle Measurement Instrument (OCA50, Dataphysics, Germany).

2.3.4. Encapsulation efficiency and loading capacity

The encapsulation efficiency (EE) and loading capacity (LC) of CA was determined by ultraviolet–visible spectrophotometer (UV-9000, Shanghai Metash Instruments Co., Ltd, Shanghai, China) according to the method of Nallamuthu.et al with some modifications (Nallamuthu, Devi, & Khanum, 2015). Briefly, the fresh nanoparticle dispersion sample were centrifuged at 40,000 g, for 30 min to obtain a supernatant containing free CA. The absorbance was measured at 327 nm. A standard curve was established for CA dissolved in aqueous medium. The encapsulation efficiency (EE) and loading capacity (LC) of the nanoparticle-loaded CA were calculated by the following formula:

EE(%)=(weight of CA in nanoparticles)/(weight of total CA) × 100.

LC(%)=(weight of CA in nanoparticles)/(weight of nanoparticles) × 100.

2.3.5. Fourier-transform infrared analysis

FTIR spectra of CS powder, TPP powder, CA powder, CS nanoparticles and CS-CA nanoparticles with the ratio of CS to CA 1:0.75 were determined according to the method of Yuan et al (Yuan, Nie, Liu, & Ren, 2021). FTIR spectra of samples were carried for evaluation of chemical interactions of functional groups by using a Fourier transform spectrophotometer (VERTEX 70, Bruker, German), at a spectral resolution of 4 cm^{-1} and in the frequency range between 400 and 4000 cm^{-1}.

2.4. Preparation of Pickering emulsion

The Pickering emulsions (40 mL) stabilized by CS nanoparticles and CS-CA particles with different ratios were prepared respectively. Cinnamaldehyde essential oil was used as the dispersed phase, and the continuous (aqueous) phase contained 0.1% w/v of particles. The pH of the aqueous phase was set at 6.9. The mixture was emulsified with a homogenizer (Ultra-Turrax Digital T25, IKA, Germany) operated at 5000 rpm and room temperature for 5 min. The oil was added progressively during the homogenization.

2.5. Characterization of Pickering emulsion

2.5.1. Optical micrographs and of Pickering emulsion

Optical micrographs of the emulsions were obtained using an optical microscope (AxioVision Release 4.8, Zeiss, Germany) fitted with a digital camera. A drop of emulsion was placed at the center of the slide glass and covered with a coverslip.

2.5.2. Droplet size and Zeta-potential measurement of Pickering emulsion

The droplet-size and Zeta-potential of Pickering emulsions were obtained by Malvern Mastersizer MS2000 (Malvern Instruments Ltd., Malvern, UK) and ZS Zetasizer Nano (4 mW He/Ne laser emitting at 633 nm), respectively. The results reported were averaged over three readings.

2.5.3. Stability analysis of Pickering emulsion

The stability of emulsions was assessed by calculating the creaming index of Pickering emulsion at first day and 5th days according to the method of Aphibanthammakit et al. (Aphibanthammakit, Barbar, Nigen, Sanchez, & Chalier, 2020). The clear liquid layer height (H_C) and total emulsion height (H_T) were measured once a day. Creaming index was calculated using the following equation:

Creaming index(%)=($H_C/H_T \times 100\%$).

2.6. Data analysis

Statistical analyses were performed using Origin (ver. 6.0, IBM software, Chicago, USA). One-way analysis of variance (ANOVA) was used to evaluate the significance of differences between sample groups at a level of $P \leq 0.05$.

3. Results and discussions

Morphology, particle size and surface charge of CA-loaded CS nanoparticles.

The morphology of the nanoparticles with different CA contents was examined by SEM and the results were shown in Fig. 1. The morphology of nanoparticles with/without CA-loaded appeared as regular spherical shapes. Compared with the particles loaded with CA, the diameter of nanoparticles without CA-loaded was more uniform. With the increase in the CA content, the particle size decreased. Moreover, the increasing of the CA content promoted nanoparticles to form heterogeneous nanoparticles.

The Z-average diameter, Zeta-potential, and PDI of CS-CA nanoparticles were shown in table 1. In comparison with the control group, the Z-average diameter of nanoparticles decreased with the increasing of CA content. The Z-average diameter of CS-CA nanoparticles after decreasing the ratios of CS to CA from1:0.25 to 1:1 were 214.7 ± 31.3 nm, 207.6 ± 29.4 nm, 189.4 ± 42.1 nm and 176.8 ± 38.5 nm, respectively. The reduction of Z-average diameter nanoparticles with increasing of the concentration CA could be a result of the large number of amino groups in CS, which leads to a large accumulation of polymer chains, which leads to interaction with CA (Nayeresadat et al., 2019). The results were in accordance with that reported by Feyzioglu who has reported small particles were obtained by encapsulating summer savory (*Satureja hortensis L.*) essential oil into CS-TPP particles (Feyzioglu, Cansu, Tornuk, & Fatih, 2016). The polydispersity index (PDI) value is a key factor in evaluation of the particle size dispersion of nanoparticles. In general, particles can be considered in monodisperse status when the PDI value is<0.3, while in polydispersity status when the PDI value is above 0.7 (Nidhin et al., 2008). In our research, the PDI values of nanoparticles with the ratios of CS to CA from1:0.25 to 1:0.75were around 0.23–0.29, suggesting that the nanoparticles were in a state of monodispersity distribution. Zeta-potential is a critical factor indicative of the colloidal stability. Specifically, the absolute value of the zeta potential above 30 mV, which is due to the electric repulsion between the particles, is indicating a stable dispersion status. In our research, as shown in table 1, the Zeta potential of CS nanoparticles was 28.8 ± 4.2, larger than that of CA-loaded. CS-CA nanoparticles after decreasing the ratios of CS to CA from 1:0.25 to 1:1 were 25.6 ± 3.2, 21.7 ± 3.1, 18.1 ± 3.8, 14.5 ± 3.7, respectively. The decrease of the absolute zeta potential values of nanopaticles with higher content of CA was considered to be caused by the interaction between CS and CA (Sotelo-Boyás, Correa-Pacheco, Bautista-BaOs, & Corona-Rangel, 2017).

3.2. Wettability of CA-loaded CS nanoparticles

The contact angles of different CA-loaded CS nanoparticles represent in Table 1. The contact angle of CS nanoparticles was 74.4 ± 0.6, while the contact angle of CA-CS nanoparticles were 76.5 ± 0.7, 80.9 ± 0.2, 82.5 ± 0.8, 84.1 ± 0.2 with decreasing the ratios of CS to CA from 1:0.25 to 1:1. The increasing of the hydrophobicity of CS-CA nanoparticles could be attributed to the fact that the interaction between the hydroxyl group of CS and the carboxyl group of CA, leading to the larger number of *N*-acetyl-d-glucosamine units (Hu, Sun, Xie, Xue, & Shao, 2020). The

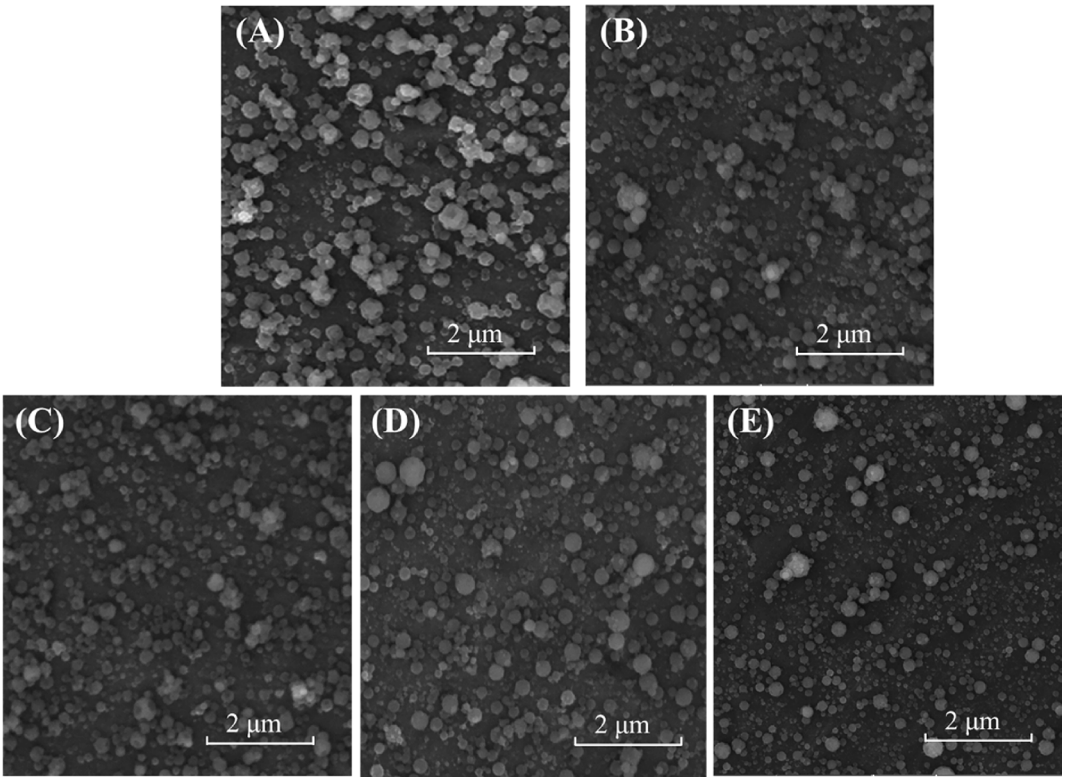

Fig.1. SEM images of (A) CS nanoparticles and CS-CA nanoparticles with different ratio CS to CA: (B) 1:0.25, (C) 1:0.5, (D) 1:0.75, (E) 1:1.

Table 1
Characterization of CA-loaded CS nanoparticles.

CS: CA	Z-average diameter (nm)	PDI	ξ-potential (mV)	EE (%)	LC (%)	Contact angle (°)
0	237.5 ± 22.7^{a}	0.232 ± 0.041^{d}	28.8 ± 4.2^{a}	–	–	74.4 ± 0.6^{e}
1:0.25	214.7 ± 31.3^{b}	0.286 ± 0.058^{b}	25.6 ± 3.2^{b}	50.47 ± 0.76^{a}	10.28 ± 1.24^{d}	76.5 ± 0.7^{d}
1:0.5	207.6 ± 29.4^{bc}	0.257 ± 0.034^{c}	21.7 ± 3.1^{c}	45.62 ± 0.87^{b}	17.17 ± 0.86^{c}	80.9 ± 0.2^{c}
1:0.75	189.4 ± 42.1^{c}	0.297 ± 0.039^{b}	18.1 ± 3.8^{d}	40.37 ± 0.65^{c}	21.58 ± 1.05^{b}	82.5 ± 0.8^{b}
1:1	176.8 ± 38.5^{d}	0.321 ± 0.049^{a}	14.5 ± 3.7^{e}	35.27 ± 1.16^{d}	24.28 ± 0.73^{a}	84.1 ± 0.2^{a}

a–e, means with different capital letters in the same column are significantly different at $p < 0.05$ according to Tukey's test.

number of these units is an important factor affecting the hydrophobicity of chitosan. When the number of these units increases, the hydrophobicity of chitosan increases (Sharkawy, Barreiro, & Rodrigues, 2020). The wettability of nanoparticles is a crucial factor affecting the type of Pickering emulsion. When the particle contact angle is<90°, it tends to form O/W emulsion, and when the particle contact angle is greater than 90°, W/O emulsion is formed. When the contact angle approaches 90°, the most stable Pickering emulsion is formed (Sharkawy, Barreiro, & Rodrigues, 2020). In our study, the contact angles of chitosan particles were close to 90°, which can be used to stabilize the emulsion.

3.3. Encapsulation efficiency and loading capacity

The encapsulation efficiency (EE) and loading capacity (LC) were analyzed to assess the suitability of the CS nanoparticles as CA delivery vehicles. As shown in Table 1, the encapsulation efficiency of CA decreased significantly ($P < 0.05$) from 50.47 ± 0.76 to 35.27 ± 1.16 upon increase in initial CA concentration. The sample with the maximum EE was obtained by using the minimum CA concentration. The limitation for encapsulating more CA was probably because the saturation of CA loaded into CS nanoparticles (Yoksan, Jirawutthiwongchai, & Arpo, 2010). As seen in Table1, the loading capacity (LC) of CA was 10.28 ± 1.24, 17.17 ± 0.86, 21.58 ± 1.05, 24.28 ± 0.73 with decreasing the ratios of CS to CA from 1:0.25 to 1:1. Contrary to EE, the LC of CA increased significantly ($P < 0.05$) with decreasing the ratios of CS to CA. The results were in agreement with that reported by AmirAmiri who also observed the decrease in EE and increase in LC when encapsulated cumin essential oil into chitosan particles (Amiri, Mousakhani-Ganjeh, Amiri, Guo, Singh, & Kenari, 2020).

3.4. FTIR spectroscopy

The FTIR spectrum of CS powder, TPP powder, CA powder, CS nanoparticles and CS-CA nanoparticles with the ratio of CS to CA 1:0.75 were shown in Fig. 2. The FTIR spectra of CS powder had the characteristic peaks at 2920 cm^{-1} (C—H), 1645 cm^{-1} (amide I), 1550 cm^{-1} (amide II) (Liu et al., 2022). In the pure CA, the broad band at 1614 cm^{-1} was related to stretching vibrations of benzene ring. The broad absorption band around 3300 cm^{-1} was corresponded to the O—H stretching vibration. The bands at 1685 cm^{-1}, 1639 cm^{-1} and 1442 cm^{-1} were assigned to C═O vibrations, C═C vibrations and olefinic C—H bending vibration, respectively (Zou, Zhang, Wang, Zhang, & Zhang, 2020). For TPP , the absorption bands at 1143 and 898 cm^{-1}

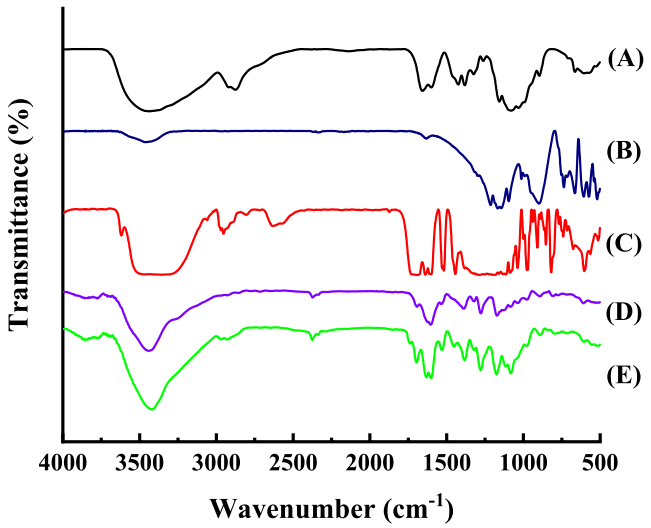

Fig. 2. FTIR spectra of (A) CS, (B) TPP, (C) CA, (D) CS nanoparticles and (E) CS-CA nanoparticles with ratio of CS to CA 1:0.75.

related to stretching vibrations of P═O groups and P—O vibrations, respectively. The typical absorption band for amide I group and amide II group at 1645 cm^{-1} and 1550 cm^{-1} observed in CS powder were shifted to 1639 cm^{-1} and 1535 cm^{-1} in CS nanoparticles which was due to the interaction of phosphate groups in TPP and amine groups in chitosan. The spectrum of CS-CA nanoparticles showed all characteristic peaks of the CS nanoparticles and CA and not any new peak was observed, this evidences that CA is successfully encapsulated into CS nanoparticles without chemical modification (Ribeiro, Roos, Ribeiro, & Nicoletti, 2020).

3.5. Morphology, droplet size and Zeta-potential of Pickering emulsion

Microscopic images of the freshly made Pickering emulsions were observed by optical microscopy. As shown in Fig. 3, the shape of droplets in all produced emulsions were spherical which was in good agreement with the previous works (Dammak and José do Amaral Sobral, 2018). This is a common case with other Pickering emulsions, as the spherical morphology results in the minimizing of the surface energy (Yang et al., 2017). The Pickering emulsion droplets appeared smaller by using nanoparticles with higher CA ratio. The uniformity of emulsion droplets was increasing stabilized by using CS-CA nanoparticles. It seems that the changes in morphology, size and distribution of emulsion droplets, resulted by the characteristics of nanoparticles (e.g., wettability, size and surface charge). These micrographic pictures and the following droplet size of the Pickering emulsions (Fig. 4) showed that the largest droplet sizes appeared in the sample stabilized by CS nanoparticles, while the droplet size of emulsion stabilized by CS-CA were 17.9 ± 2.1, 15.2 ± 3.4, 14.7 ± 3.2, 14.3 ± 4.5 with decreasing the ratios of CS to CA from 1:0.25 to 1:1, respectively. The results were in accordance with Hasanein who has prepared Rutin-loaded Pickering emulsion with the droplet size ranged between 5.8 ± 1.1 and 18.7 ± 3.4 μm (Hasanein et al., 2017). It should be noted, the Z-average diameter of CS-CA nanoparticles after decreasing the ratios of CS to CA from1:0.25 to 1:1 were 214.7 ± 31.3 nm, 207.6 ± 29.4 nm, 189.4 ± 42.1 nm and 176.8 ± 38.5 nm. The droplet size of emulsion was decreased with the diameter decreasing of nanoparticles. Generally speaking, the diameter of emulsion droplets increases as the diameter of particles adsorbed on the oil–water interface increased. Larger particles have a longer adsorption time at the oil–water interface, resulting in an increase in the diameter of the emulsion droplets (Tsabet & Fradette, 2015).

Zeta potential can be used to characterize the charge on the surface of emulsion droplets. The zeta potential of emulsion stabilized by CS

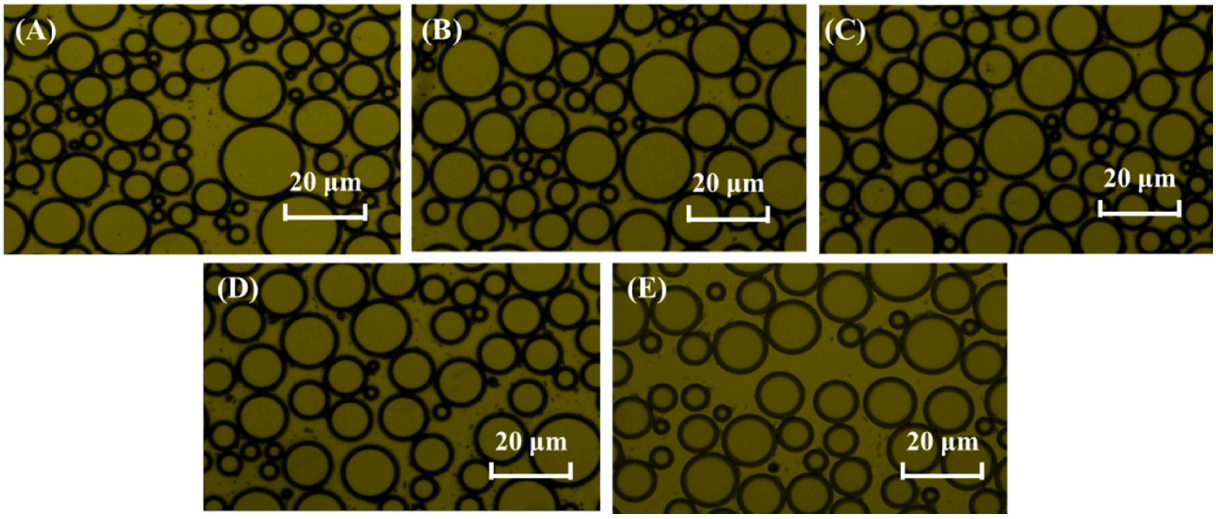

Fig. 3. Optical micrographs of emulsion stabilized by (A) CS nanoparticles and CS-CA nanoparticles with different ratio CS to CA: (B) 1:0.25, (C) 1:0.5, (D) 1:0.75, (E) 1:1.

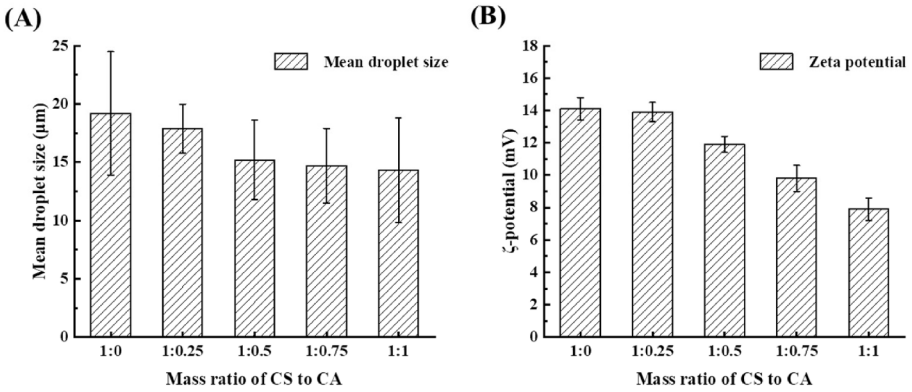

Fig. 4. Mean droplet size (A) and ζ-potential (B) of Pickering emulsion stabilized by CS nanoparticles and CS-CA nanoparticles.

nanoparticles and CS-CA nanoparticles with different ratios of CS to CA were shown in Fig. 4. The Zeta potential of emulsions were 14.1 ± 0.7, 13.9 ± 0.6, 11.9 ± 0.5, 9.8 ± 0.8, 7.9 ± 0.7 with decreasing the ratios of CS to CA from 1:0.25 to 1:1, implying a positively charged surface of the droplets. The absolute value of the Zeta potential of the emulsions gradually decreased with the increase of encapsulation efficiency and loading capacity of CS-CA nanoparticles. This may due to the encapsulation of CA introduced negatively charged carboxyl groups. As the encapsulation of CA increased, the charge density of the particle adsorption layer on the surface of the droplet decreased, and the absolute value of the ζ-potential increased accordingly (Pang, Liu, & Zhang, 2021).

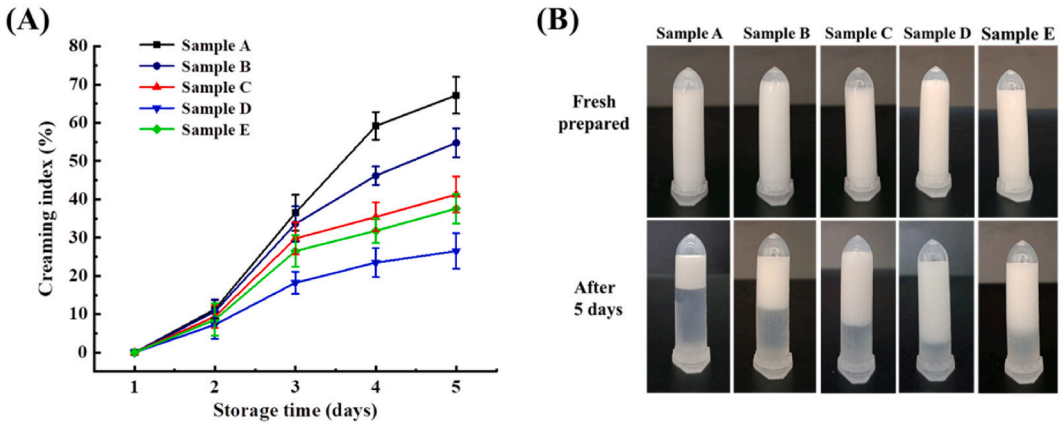

Fig. 5. Creaming index (A) and images (B) of Pickering emulsions stabilized by CS nanoparticles (Sample A) and CS-CA nanoparticles with different ratio of CS to CA. Sample B: 1:0.25, Sample C: 1:0.5, Sample D: 1:0.75, Sample E: 1:1 during storage (5 days).

3.6. Stability of Pickering emulsion

The creaming index, expressed as the height of clear liquid layer to height of total emulsion, was an indicator for assessing the stability of the emulsions. The creaming index and images of emulsions stabilized by CS nanoparticles and CS-CA nanoparticles with different ratios of CS to CA were shown in Fig. 5. As can be seen, phase separation of emulsion occurred after storage for 5 days. However, the degree of phase separation of emulsions stabilized by different particle was different significantly. The emulsion stabilized by CS-CA nanoparticles with the ratios of CS to CA 1:0.75 showed the best stability with the minimum creaming index value of 26.5 ± 4.6% after 5 days of storage. There are many reasons for this result. The stability of Pickering emulsion is affected by many factors, and it is not determined by any one of them alone, it needs to be considered comprehensively. Firstly, the contact angle is an important factor affecting the stability of emulsion. In our research, the contact angle of CS-CA nanoparticles with the ratios of CS to CA 1:0.75 was 82.5 ± 0.8°, which was only 1.6° lower than the contact angle of CS-CA nanoparticles with the ratios of CS to CA 1:1. Generally speaking, when the contact angle is close to 90°, the most stable Pickering emulsion is formed (Alehosseini, Jafari, & Shahiri Tabarestani, 2021). However, the emulsion stabilized by CS-CA nanoparticles with the ratios of CS to CA 1:0.75 showed better stability than that stabilized by CS-CA nanoparticles with the ratios of CS to CA 1:1, which might be related to the ζ-potential of emulsion. The emulsion with low ζ-potential has poor stability due to lack of strong repulsion to aggregation (Cui et al., 2021).

4. Conclusions

In the present study, CEO and CA were co-encapsulated in CS nanoparticles stabilized Pickering emulsion system. Different amount of CA was encapsulated into CS nanoparticles. The Z-average diameter and zeta potential decreased with the increase of CA content. The improvement of the wettability of nanoparticles with decreasing the ratios of CS to CA can be attributed to the fact that the interaction between the hydroxyl group of CS and the carboxyl group of CA, which is helpful to stabilize the emulsion. The Pickering emulsion system stabilized by CS-CA nanoparticles with different ratios of CS to CA was prepared. The stability of emulsions stabilized by different particle was different significantly. The emulsion stabilized by CS-CA nanoparticles with the ratios of CS to CA 1:0.75 showed the best stability with the minimum creaming index value of 26.5 ± 4.6% after 5 days of storage. The overall results presented in this work demonstrate, for the first time, the potential of CS nanoparticles stabilized Pickering emulsion system for the co-encapsulation of CEO and CA.

Declaration of Competing Interest

The authors declare that they have no known competing financial interests or personal relationships that could have appeared to influence the work reported in this paper.

Acknowledgements

This work was supported by National Natural Science Foundation of China (No. 32102048), Zhejiang province key research and development program, China (No. 2021C02015) and Zhejiang Province Natural Science Foundation of China (No. LQ22C200021). We confirm that there is no conflict of interest.

References

Alehosseini, E., Jafari, S. M., & Shahiri Tabarestani, H. (2021). Production of d-limonene-loaded Pickering emulsions stabilized by chitosan nanoparticles. *Food Chemistry, 354*, Article 129591.

Amiri, A., Mousakhani-Ganjeh, A., Amiri, Z., Guo, Y. G., Singh, A. P., & Kenari, R. E. (2020). Fabrication of cumin loaded-chitosan particles: Characterized by molecular, morphological, thermal, antioxidant and anticancer properties as well as its utilization in food system. *Food Chemistry, 310*, Article 125821.

Aphibanthammakit, C., Barbar, R., Nigen, M., Sanchez, C., & Chalier, P. (2020). Emulsifying properties of Acacia senegal gum: Impact of high molar mass protein-rich AGPs. *Food Chemistry: X, 6*, Article 100090.

Cao, H., Saroglu, O., Karadag, A., Diaconeasa, Z., Zoccatelli, G., Conte-Junior, C., … Xiao, J. (2021). Available technologies on improving the stability of polyphenols in food processing. *Food Frontiers, 2*, 109–139.

Cui, F., Zhao, S., Guan, X., McClements, D. J., Liu, X., Liu, F., & Ngai, T. (2021). Polysaccharide-based Pickering emulsions: Formation, stabilization and applications. *Food Hydrocolloids, 119*, Article 106812.

Dammak, I., & José do Amaral Sobral, P. (2018). Formulation optimization of lecithin-enhanced pickering emulsions stabilized by chitosan nanoparticles for hesperidin encapsulation. *Journal of Food Engineering, 229*, 2-11.

Feyzioglu, Cansu, G., Tornuk, & Fatih. (2016). Development of chitosan nanoparticles loaded with summer savory (Satureja hortensis L.) essential oil for antimicrobial and antioxidant delivery applications. *LWT - Food Science & Technology, 70*, 104-110.

Gao, H., Fang, X., Chen, H., Qin, Y., Xu, F., & Jin, T. Z. (2017). Physiochemical properties and food application of antimicrobial PLA film. *Food Control, 73*, 1522–1531.

Hasanein, M., Asfour, H., Elmotasem, M., & D., Mostafa, Abeer, A. A., & Salama. (2017). Chitosan based Pickering emulsion as a promising approach for topical application of rutin in a solubilized form intended for wound healing: In vitro and in vivo study. *International journal of pharmaceutics, 534*, 325–338.

Ho, K. W., Ooi, C. W., Mwangi, W. W., Leong, W. F., Tey, B. T., & Chan, E.-S. (2016). Comparison of self-aggregated chitosan particles prepared with and without ultrasonication pretreatment as Pickering emulsifier. *Food Hydrocolloids, 52*, 827–837.

Hu, F., Sun, T., Xie, J., Xue, B., & Shao, Z. (2020). Functional properties and preservative effect on Penaeus vannamei of chitosan films with conjugated or incorporated chlorogenic acid. *International Journal of Biological Macromolecules, 159*, 333–340.

Jiang, B., Liu, R., Fang, X., Tong, C., Chen, H., & Gao, H. (2022). Effects of salicylic acid treatment on fruit quality and wax composition of blueberry (Vaccinium virgatum Ait). *Food Chemistry, 368*, Article 130757.

Jiao, W., Shu, C., Li, X., Cao, J., Fan, X., & Jiang, W. (2019). Preparation of a chitosan-chlorogenic acid conjugate and its application as edible coating in postharvest preservation of peach fruit. *Postharvest Biology and Technology, 154*, 129–136.

Lin, Y., Lin, Y., Lin, M., Fan, Z., & Lin, H. (2021). Influence of hydrogen peroxide on the ROS metabolism and its relationship to pulp breakdown of fresh longan during storage. *Food Chemistry: X, 12*, Article 100159.

Liu, J., Song, F., Chen, R., Deng, G., Chao, Y., Yang, Z., … Hu, Y. (2022). Effect of cellulose nanocrystal-stabilized cinnamon essential oil Pickering emulsions on structure and properties of chitosan composite films. *Carbohydrate Polymers, 275*, Article 118704.

Liu, R., Gao, H., Chen, H., Fang, X., & Wu, W. (2019). Synergistic effect of 1-methylcyclopropene and carvacrol on preservation of red pitaya (Hylocereus polyrhizus). *Food Chemistry, 283*, 588–595.

Liu, S., Yang, Q., Zhang, J., Yang, M., Wang, Y., Sun, T., … Abd El-Aty, A. M. (2022). Enhanced stability of stilbene-glycoside-loaded nanoparticles coated with carboxymethyl chitosan and chitosan hydrochloride. *Food Chemistry, 372*, Article 131343.

Nallamuthu, I., Devi, A., & Khanum, F. (2015). Chlorogenic acid loaded chitosan nanoparticles with sustained release property, retained antioxidant activity and enhanced bioavailability. *Asian Journal of Pharmaceutical Sciences, 10*(3), 203–211.

Nayeresadat, H., Faramarz, K., & Mohammad, & Safari. (2019). Improving the antifungal activity of clove essential oil encapsulated by chitosan nanoparticles. *Food Chemistry, 275*, 113–122.

Nidhin, I., Sreeram, B., & Unni, & Nair. (2008). Synthesis of iron oxide nanoparticles of narrow size distribution on polysaccharide templates. *Bulletin of Materials Science, 31*, 93–96.

Niu, B., Shao, P., & Sun, P. (2019). Ultrasound-assisted emulsion electrosprayed particles for the stabilization of β-carotene and its nutritional supplement potential. *Food Hydrocolloids, 102*, Article 105634.

Pang, B., Liu, H., & Zhang, K. (2021). Recent progress on Pickering emulsions stabilized by polysaccharides-based micro/nanoparticles. *Advances in Colloid and Interface Science, 296*, Article 102522.

Rattanaburi, P., Charoenrat, N., Pongtharangkul, T., Suphantharika, M., & Wongkongkatep, J. (2019). Hydroxypropyl methylcellulose enhances the stability of o/w Pickering emulsions stabilized with chitosan and the whole cells of Lactococcus lactis IO-1. *Food Research International, 116*, 559–565.

Ribeiro, E. F., de Barros-Alexandrino, T. T., Assis, O. B. G., Junior, A. C., Quiles, A., Hernando, I., & Nicoletti, V. R. (2020). Chitosan and crosslinked chitosan nanoparticles: Synthesis, characterization and their role as Pickering emulsifiers. *Carbohydrate Polymers, 250*, Article 116878.

Ribeiro, M. L. F. F., Roos, Y. H., Ribeiro, A. P. B., & Nicoletti, V. R. (2020). Effects of maltodextrin content in double-layer emulsion for production and storage of spray-dried carotenoid-rich microcapsules. *Food and Bioproducts Processing, 124*, 208–221.

Sharkawy, A., Barreiro, M. F., & Rodrigues, A. E. (2020). Chitosan-based Pickering emulsions and their applications: A review. *Carbohydrate Polymers, 250*, Article 116885.

Sotelo-Boyás, M. E., Correa-Pacheco, Z. N., Bautista-BaOs, S., & Corona-Rangel, M. L. (2017). Physicochemical characterization of chitosan nanoparticles and nanocapsules incorporated with lime essential oil and their antibacterial activity against food-borne pathogens. *LWT- Food Science and Technology, 77*, 15–20.

Tsabet, È., & Fradette, L. (2015). Effect of the properties of oil, particles, and water on the production of Pickering emulsions. *Chemical Engineering Research and Design, 97*, 9–17.

Valeria, C., Manuela, V., Alessandra, B., Marco, D., Irene, M., Maurizia, D., & Maria, D. (2019). *In vivo Modulatory Effect of Coffee (Coffea canephora var. Robusta) on the Expression Levels of Murine microRNA-124-3p Associated with Antioxidant Defenses., eFood, 1*, 140–146.

Xia, T., Xue, C., & Wei, Z. (2021). Physicochemical characteristics, applications and research trends of edible Pickering emulsions. *Trends in Food Science & Technology, 107*, 1–15.

Yang, Y., Fang, Z., Chen, X., Zhang, W., Xie, Y., Chen, Y., … Yuan, W. (2017). An Overview of Pickering Emulsions: Solid-Particle Materials, Classification, Morphology, and Applications. *Frontiers in Pharmacology, 8*, 287.

Yoksan, R., Jirawutthiwongchai, J., & Arpo, K. (2010). Encapsulation of ascorbyl palmitate in chitosan nanoparticles by oil-in-water emulsion and ionic gelation processes. *Colloids & Surfaces B Biointerfaces, 76*, 292–297.

Yuan, E., Nie, S., Liu, L., & Ren, J. (2021). Study on the interaction of Hericium erinaceus mycelium polysaccharides and its degradation products with food additive silica nanoparticles. *Food Chemistry: X, 12*, Article 100172.

Zou, Y., Zhang, C., Wang, P., Zhang, Y., & Zhang, H. (2020). Electrospun chitosan/polycaprolactone nanofibers containing chlorogenic acid-loaded halloysite nanotube for active food packaging. *Carbohydrate Polymers, 247*, Article 116711.